

## SrTiO<sub>3</sub>:Cr nanocrystalline powders: size effects and optical properties

This article has been downloaded from IOPscience. Please scroll down to see the full text article.

2009 J. Phys.: Condens. Matter 21 375303

(<http://iopscience.iop.org/0953-8984/21/37/375303>)

View [the table of contents for this issue](#), or go to the [journal homepage](#) for more

Download details:

IP Address: 129.252.86.83

The article was downloaded on 30/05/2010 at 05:01

Please note that [terms and conditions apply](#).

# SrTiO<sub>3</sub>:Cr nanocrystalline powders: size effects and optical properties

V A Trepakov<sup>1,2</sup>, Z Potůček<sup>1,3,5</sup>, M V Makarova<sup>1</sup>, A Dejneka<sup>1</sup>,  
P Szama<sup>4</sup>, L Jastrabik<sup>1</sup> and Z Bryknař<sup>3</sup>

<sup>1</sup> Institute of Physics ASCR, v. v. i., Na Slovance 2, CZ-182 21 Praha 8, Czech Republic

<sup>2</sup> A F Ioffe Physico-Technical Institute RAS, 194 021, Saint Petersburg, Russia

<sup>3</sup> Faculty of Nuclear Sciences and Physical Engineering, Czech Technical University in Prague, Trojanova 13, CZ-120 00 Praha 2, Czech Republic

<sup>4</sup> J Heyrovsky Institute of Physical Chemistry AS CR, v. v. i., Dolejškova 2155/3, CZ-182 23 Praha 8, Czech Republic

E-mail: [potucek@fzu.cz](mailto:potucek@fzu.cz)

Received 9 June 2009

Published 19 August 2009

Online at [stacks.iop.org/JPhysCM/21/375303](http://stacks.iop.org/JPhysCM/21/375303)

## Abstract

The crystal structure, optical absorption, and photoluminescence of chromium impurity centers were studied in nanocrystalline SrTiO<sub>3</sub>:Cr (0.1 mol%) powders with average particle size within the range 13–100 nm prepared by the Pechini-type polymeric sol–gel method. Only the presence of a cubic perovskite phase of O<sub>h</sub><sup>1</sup> symmetry was proved for the powders at room temperature, by means of x-ray diffraction. The lattice constant  $a = 3.910$  Å, larger than that of bulk SrTiO<sub>3</sub> crystals ( $a = 3.905$  Å), was found for nanoparticles with the size about 20 nm. The optical absorption edge and the zero-phonon R-line (<sup>2</sup>E → <sup>4</sup>A<sub>2</sub>) of luminescence of the octahedral Cr<sup>3+</sup> centers shifted to higher energies with decreasing nanoparticle size. These size effects were regarded as intrinsic to SrTiO<sub>3</sub>. An unusual and large temperature shift of the R-line position very similar to the ‘dielectric related’ one of the bulk crystals was observed for all powders, evidencing their quantum paraelectric behavior. However, the powders with the average particle size about 13 and 20 nm did not reveal completely reproducible behavior of the R-line position at low temperatures. This instability was considered a possible manifestation of a low-temperature phase transition in small enough SrTiO<sub>3</sub> nanoparticles.

## 1. Introduction

The study of the size effects in quantum paraelectric SrTiO<sub>3</sub> (STO), the most popular and widely investigated model material from the perspective of the ABO<sub>3</sub> perovskite-like oxides and phase transition physics, is of great interest. At  $T \approx 105$  K, STO undergoes an antiferrodistortive structural phase transition between the cubic O<sub>h</sub><sup>1</sup> and tetragonal D<sub>4h</sub><sup>18</sup> phases. The dielectric permittivity strongly rises on cooling with an extrapolated Curie–Weiss temperature  $T_c \approx 35$  K and the lowest TO<sub>1</sub> phonon mode softens. However, at the lowest temperatures the dielectric permittivity saturates and the trend to ferroelectric ordering is suppressed due to quantum mechanical effects (quantum paraelectricity) [1]. Nevertheless, even low levels of appropriate impurities or perturbations can induce in STO a phase transition associated

with considerable changes of physical properties. These features result in remarkable properties of STO including a very unusual and large temperature shift of the zero-phonon R-line of luminescence of octahedral Cr<sup>3+</sup> impurity centers corresponding to the <sup>2</sup>E → <sup>4</sup>A<sub>2</sub> emission transition [2]. For the tetragonal D<sub>4h</sub><sup>18</sup> phase the R-line splitting to a doublet was observed and the temperature shift  $\Delta\nu$  of the average position of the R-lines was found proportional to the reciprocal dielectric constant  $1/\epsilon'$ , i.e.  $\Delta\nu \sim 1/\epsilon' \sim \omega_0^2$  where  $\omega_0^2$  is a frequency of the TO<sub>1</sub> soft phonon mode. Such temperature behavior of the R-line position was assigned to interaction of the impurity centers with the lowest-frequency temperature dependent TO<sub>1</sub> phonon branch [2] and, microscopically, to local configurational instability of the 3d<sup>3</sup> impurity centers in the orbitally degenerate <sup>2</sup>E state due to the Jahn–Teller effect on the soft TO<sub>1</sub> phonon mode [3]. This ‘dielectric related’ temperature shift of the R-line allows successive use of Cr<sup>3+</sup> ions as a luminescent spectroscopic probe in studies of TO

<sup>5</sup> Author to whom any correspondence should be addressed.

phonon mode behavior and phase transitions, as was proved for  $\text{Sr}_{1-x}\text{Ca}_x\text{TiO}_3$  [4]. Being encouraged by this result, we tried to study size effects in STO nanoparticles by means of the luminescence of  $\text{Cr}^{3+}$  ions.

In this work we report on the preparation of nanocrystalline STO:Cr (0.1 mol%) powders and the results of a study of the optical absorption and photoluminescence of  $\text{Cr}^{3+}$  ions in STO nanoparticles. To our knowledge, the photoluminescence of nanocrystalline STO:Cr particles has been reported earlier only in [5] where the main attention was paid to the shape, position, and lifetime of the  $\text{Cr}^{3+}$  emission R-line in the vicinity of the antiferrodistortive structural phase transition temperature.

## 2. Experimental details

The synthesis of the yellow tinted nanocrystalline STO:Cr (0.1 mol%) powders was based on the Pechini-type polymeric sol-gel method described in [6]. In this method homogeneous distribution of cations is achieved by the formation of polymeric complexes of Sr, Ti, and Cr ions with citric acid and ethylene glycol. This approach allows one to decrease the temperature of the STO phase formation in comparison to the conventional solid state methods and to obtain nanocrystalline powders with average particle sizes of about 13 and 20 nm. The synthesis was performed in the following steps: (i)  $\text{TiO}_2 \cdot x\text{H}_2\text{O}$  was prepared by hydrolysis of  $\text{TiCl}_4$  with distilled water and then with a 25% water solution of  $\text{NH}_3$ ; (ii)  $\text{Cl}^-$  ions were removed from the precipitate by washing with water; (iii) the fresh precipitate was dissolved in citric acid and the Ti content was determined; (iv) specific amounts of  $\text{Sr}(\text{NO}_3)_2$ ,  $\text{Cr}(\text{NO}_3)_3 \cdot 9\text{H}_2\text{O}$ , and citric acid were dissolved and added to the solution of citric acid containing Ti; (v) a polymeric gel was formed by addition of the ethylene glycol to the solution and solvent was evaporated; (vi) the polymeric gel obtained was pyrolyzed and annealed for 1 h at 400 °C. Additional annealing of the synthesized STO:Cr powder with the average particle size of about 20 nm for 1 h at 750 and 900 °C allowed us to increase the average particle sizes to 50 and 100 nm, respectively. The nominally pure STO powder with the average particle size of about 1000 nm was prepared by grinding of the Verneuil grown STO single crystals.

The average particle size of the prepared STO:Cr powders was estimated by the analysis of SEM micrographs and from the coherent domain size assessed from the broadening of XRD peaks. An example of an SEM micrograph in figure 1 obtained for the STO:Cr powder with the average particle size about 20 nm demonstrates rather prolate shape of the nanoparticles. The SEM micrographs and XRD patterns were obtained using the SEM micrograph Hitachi S-4800 and a Bruker D8 Advance powder x-ray diffractometer with a Vantec-1 detector and  $\text{Cu K}\alpha$  radiation, respectively. The lattice constant was determined by fitting of the XRD pattern by the method of least squares using the RIETAN software package.

The diffuse reflectance spectra were recorded at room temperature using the Perkin-Elmer Lambda 19 UV-vis-NIR spectrophotometer equipped with an integrating sphere. The

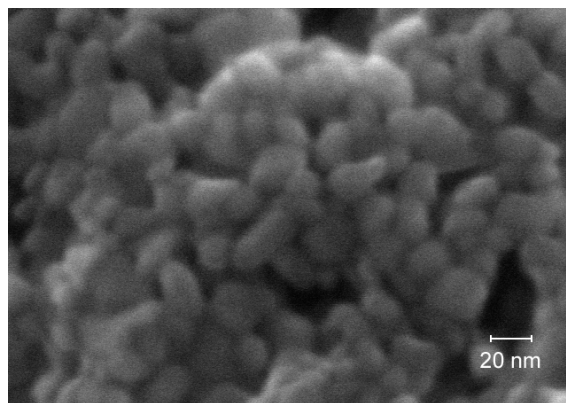


**Figure 1.** SEM micrograph of the nanocrystalline STO:Cr powder with the average particle size about 20 nm.

$\text{BaSO}_4$  plate was used as a reference standard. The measured spectra were transformed according to the Schuster-Kubelka-Munk theory in order that quantitative evaluations could be performed. The ratio  $F(R_\infty)$  of the absorption coefficient  $K$  to the scattering coefficient  $S$ , called the ‘absorbance’ or Kubelka-Munk function, can be expressed as

$$F(R_\infty) = \frac{K}{S} = \frac{(1 - R_\infty)^2}{2R_\infty}$$

where  $R_\infty$  is the reflectance measured as the ratio of the total intensities of light reflected from the sample and from the standard [7]. The absorbance  $F(R_\infty)$  obtained for the STO:Cr powders has similar spectral behavior to the optical absorption.

The photoluminescence emission spectra of the powder loosely filled into the cavity of a copper holder fixed to a finger of a closed-cycle helium refrigerator were measured in the temperature region 12–300 K using a set-up equipped with the McPherson 2061 grating monochromator and cooled RCA 31034 photomultiplier (GaAs photocathode) operating in the photon-counting mode. Photoluminescence was excited with light of a high-pressure xenon lamp filtered through a double-grating monochromator (Jobin-Yvon DH 10 UV). All emission spectra were corrected for the spectral response of the apparatus.

## 3. Results and discussion

Analysis of XRD patterns proved only the presence of a single phase with  $\text{O}_h^1$  cubic perovskite structure in the powders at room temperature. An example of an XRD pattern illustrating this result for the STO:Cr powder with the average particle size about 20 nm is shown in figure 2. Thorough determination of the lattice constant performed on the powder with the average particle size about 20 nm revealed the magnitude  $a = 3.910 \pm 0.002 \text{ \AA}$  which is larger than for the bulk STO crystals ( $a = 3.905 \text{ \AA}$  [8]). At first glance, the lattice expansion looks rather unexpected for small nanoparticles due to the increasing compressive stress in the particles caused by surface tension. At the same time, the monotonic increase of the lattice constant was also recently observed for nanocrystalline

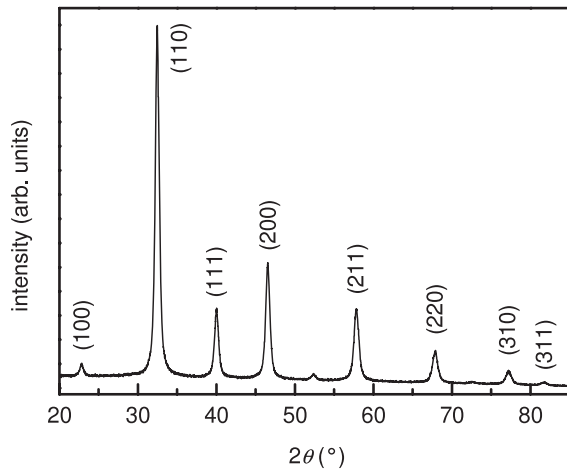


**Figure 2.** XRD pattern of the nanocrystalline STO:Cr powder with the average particle size about 20 nm. The Miller indices are assigned to the XRD peaks of STO.

STO particles with decrease in their size from 40 to 12 nm and was ascribed to the negative pressure effect due to the enhanced surface-defect dipoles [9]. However, the increase of the lattice constant for nanoparticles with the size about 20 nm was in our case approximately two times smaller than in [9]. We suppose that this discrepancy could be caused by differences in composition of the nanoparticles as a result of different techniques of preparation that can particularly influence the content of hydroxyl (OH) groups. The noticeable lattice expansion attributed to the presence of OH groups was observed for (Sr, Na)ZrO<sub>3</sub> nanoparticles with the size about 40 nm where annealing at temperatures higher than 300 °C led to water elimination and decrease in the lattice constant conspicuously independent of the annealing temperature up to 1000 °C [10]. The nanocrystalline STO particles studied

in [9] were prepared by hydrolysis and so they could contain hydroxyl groups in the bulk. Since increase in the nanoparticle size from 12 to 40 nm was achieved in [9] by elevation of the annealing temperature from 450 to 800 °C the formation of smaller nanoparticles could be accompanied by lower water loss in the samples and in consequence by the observed considerable increase of the lattice constant due to the higher content of OH groups. In contrast, the probability of hydroxyl group inclusion into our STO:Cr powder with the average particle size about 20 nm prepared by pyrolysis of polymeric citrate gel should be low. Therefore the influence of hydroxyl groups on the observed increase of the lattice parameter in comparison with the bulk STO crystals is suppressed and we deal with a weaker intrinsic effect.

Figure 3 shows the spectral dependence of the absorbance  $F(R_\infty)$  for the nominally pure STO powder with the average particle size about 1000 nm and nanocrystalline STO:Cr powders with various particle size taken at room temperature. The spectra clearly demonstrate at least two size effects. First of all, the optical absorption edge obviously shifts to higher energies with decreasing particle size. The optical band-gap energy of 3.22 eV, consistent with a conventional onset of the interband optical transitions quoted for STO crystals at room temperature [11, 12], was obtained for the nominally pure STO powder with the average particle size about 1000 nm from rough estimation at the absorbance level  $F(R_\infty) = 0.2$ . Then fixing this absorbance level, a progressively increasing band-gap energy of 3.34, 3.39, and 3.41 eV was found in the STO:Cr powders with the average particle sizes of about 100, 20, and 13 nm. This result is qualitatively consistent but quantitatively considerably different in comparison with the recently observed increase of the band-gap energy with decreasing size of nanocrystalline STO particles up to  $\sim 3.61$  eV for nanoparticles with size of about 12 nm that was

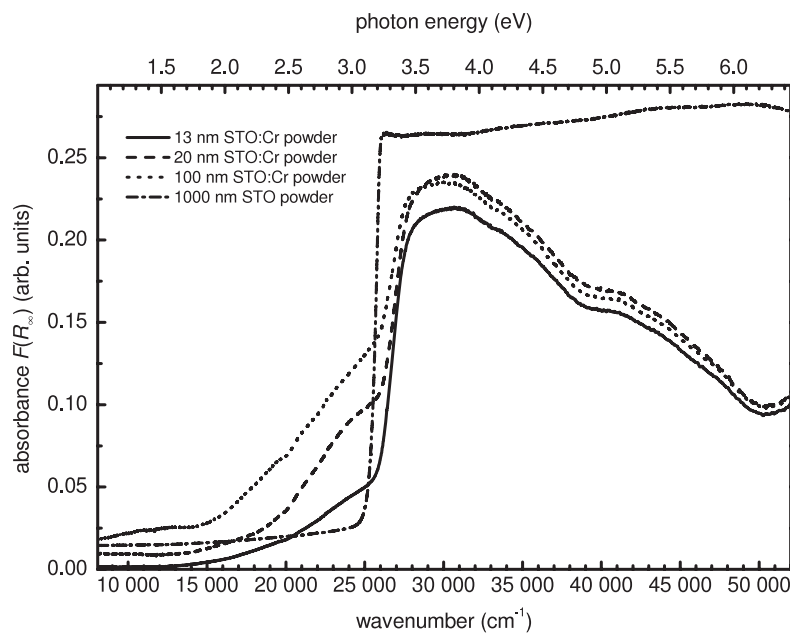


**Figure 3.** Spectral dependence of the absorbance  $F(R_\infty)$  for the nominally pure STO powder with average particle size of about 1000 nm and the nanocrystalline STO:Cr powders with average particle sizes of about 13, 20, and 100 nm.

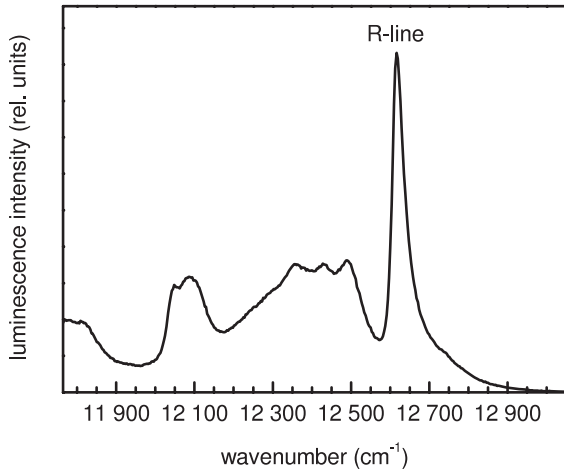


**Figure 4.** Photoluminescence emission spectrum of the nanocrystalline STO:Cr powder with the average particle size of about 20 nm. Photoluminescence was excited with 465 nm light at 20 K.

reported in [9]. We believe that the considerable increase of the band-gap energy reported in [9] is substantially influenced by the presence of hydroxyl groups in the STO nanoparticles and the related increase of the lattice constant discussed above. On the other hand, the content of OH groups in our nanocrystalline STO:Cr particles prepared by pyrolysis of polymeric citrate gel is negligible and the increase of the band-gap energy with decreasing nanoparticle size observed here is an intrinsic effect that is less pronounced than that reported in [9]. Such band-gap behavior is rather remarkable

for the STO nanoparticles of actual size and can be connected to narrowing of the lowest  $d_\epsilon$  conduction band and the upper  $2p$  valence band [13] due to the increasing lattice constant and decreasing size of the nanoparticles themselves. The second effect is the development of the absorption tail below the absorption edge of the nanocrystalline STO:Cr powders, that can be tentatively attributed to nanoparticle inhomogeneities. Finally, the pronounced decrease of optical absorption of the nanocrystalline STO:Cr powders in comparison with the nominally pure STO powder with average particle size of about 1000 nm is evident in the spectral region of the deep interband transitions. An explanation of the nature of this effect needs further investigation.

All of our nanocrystalline STO:Cr powders revealed photoluminescence of  $\text{Cr}^{3+}$  ions in the near infrared spectral region very similar to that of the bulk STO:Cr crystals [2]. The emission spectrum consists of the zero-phonon R-line corresponding to the  ${}^2E \rightarrow {}^4A_2$  transition of octahedral  $\text{Cr}^{3+}$  centers and vibronic sidebands (see figure 4). The R-line appeared to be rather inhomogeneously broadened for all our powders; for instance, for the powder with the average particle size of about 100 nm its half-width was  $\sim 22 \text{ cm}^{-1}$  at 20 K. This broadening hampered observation of the R-line splitting in the tetragonal  $D_{4h}^{18}$  phase. The width of the R-line increased with decreasing nanoparticle size in a similar way like in [5]. Figure 5 presents the temperature dependence of the R-line position for STO:Cr crystals and nanocrystalline powders with various particle sizes. The R-line position in the STO:Cr powders is obviously shifted to higher energies in comparison with its position for single crystals and this shift evidently tends to increase with decreasing nanoparticle size. Such ‘blue’

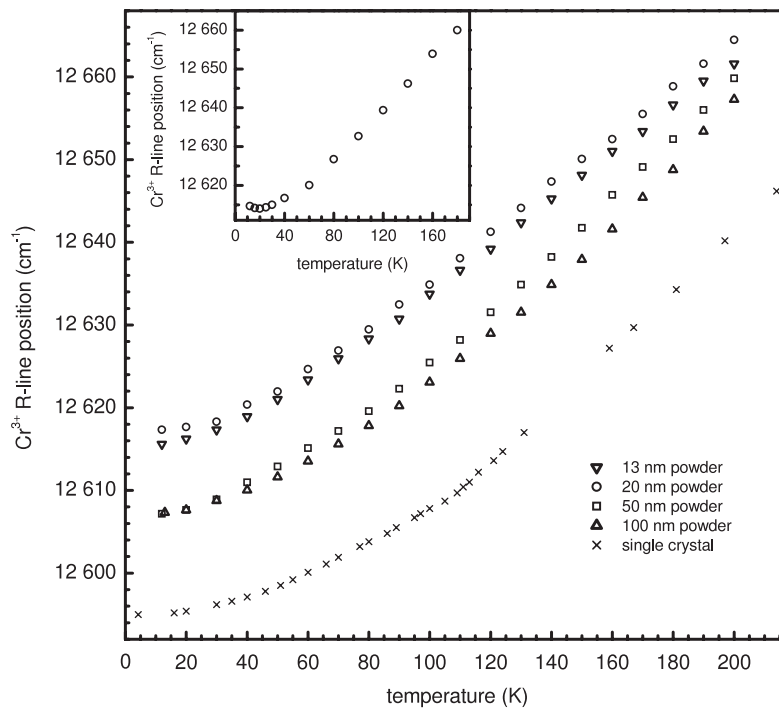


**Figure 5.** Temperature dependence of the average position of the R-line of  $\text{Cr}^{3+}$  emission for STO:Cr single-crystal and nanocrystalline powders with the average particle sizes of about 13, 20, 50, and 100 nm. Photoluminescence of STO:Cr powders was excited with 465 nm light. The single-crystal data set was taken from [2]. The inset illustrates the instability of the temperature dependence of the R-line position occasionally observed for powder with the average particle size about 20 nm.



shift of the R-line disagrees with findings in [5] where the shift of the R-line position to lower energies was observed for nanocrystalline STO:Cr samples and its magnitude was noticeably dependent on temperature. Since according to [14] the  ${}^2E$  level of  $\text{Cr}^{3+}$  ions is localized in STO very close ( $\sim 300$  meV) below the bottom of the conduction band, the ‘blue’ shift of the R-line position could be a consequence of a coupling of the  ${}^2E$  level with the bottom of the conduction band whose energy increases with decreasing nanoparticle size.

The character of the R-line shift to lower energies with decreasing temperature appeared to be for all nanocrystalline STO:Cr powders very similar to that of the bulk crystals [2], which evidences their quantum paraelectric behavior. However, in the case of the powders with the average particle sizes of about 13 and 20 nm the temperature dependence of the R-line position was not always completely reproducible at low temperatures and even a distinct minimum occasionally emerged near 19 K, as the inset in figure 5 clearly illustrates. Following ideas of [4], the appearance of this instability and low-temperature minimum can be considered as a manifestation of a possible low-temperature ferroelectric phase transition. The emergence of such a phase transition in small enough STO nanoparticles is not too surprising and can be connected to an increasing contribution of the surface whose phase transition temperature can be higher than that in the bulk [15] and to nanoparticle inhomogeneity with a phase transition in the framework of the percolation scenario. An important role also plays the observed increase of the lattice constant, and possible related tensile strains can promote the appearance of a ferroelectric state in STO nanoparticles as well [16, 17]. The formation of a conventional bulk polar state in small STO nanoparticles does not look very plausible due to depolarization field effects. However, the depolarization effects can be eliminated by the formation of a closed configuration of spontaneous polarization in the form of a vortex, as was considered long ago by Kittel for small ferromagnetic particles [18] or recently by Naumov and Bratkovsky for ferroelectric nanoparticles [19]. Unfortunately, insufficient reproducibility of the low-temperature minimum in the temperature dependence of the R-line energy position allows us, for now, only to claim that structural instability increases in small enough STO nanoparticles at the lowest temperatures.

#### 4. Conclusions

Nanocrystalline STO:Cr (0.1 mol%) powders with average particle sizes within the range 13–100 nm were successfully synthesized by the Pechini-type polymeric sol–gel method. The size effects considered as intrinsic ones were observed. First, a small increase of the lattice constant was found in the small STO nanoparticles. Second, decrease of the particle size was accompanied by a shift of the optical absorption edge and the position of the R-line of photoluminescence of the octahedral  $\text{Cr}^{3+}$  centers to higher energies. These shifts have been related to the lattice constant increase and to narrowing of the lowest  $d_g$  conduction band and the upper  $2p$  valence band in the STO:Cr nanoparticles. On

cooling, the R-line continuously shifted to lower energies for all STO:Cr powders nearly like in the case of the bulk crystals, which evidences conservation of quantum paraelectric behavior in the nanocrystalline powders studied. However, the powders with the average particle sizes of about 13 and 20 nm demonstrated certain instability of the R-line position behavior at low temperatures. Such instability, together with the occasional appearance of a low-temperature minimum in the temperature dependence of the R-line energy position, have been speculated to be possible manifestations of structural instability and perhaps even of a low-temperature ferroelectric phase transition for the sufficiently small STO:Cr nanoparticles.

#### Acknowledgments

This research was supported by the projects KAN301370701, AV0Z10100522, and KJB100100703 of the Academy of Sciences of the Czech Republic, by the grant 202/08/1009 of the Grant Agency of the Czech Republic, by the projects 1M06002 and MSM6840770021 of the Ministry of Education, Youth and Sports of the Czech Republic, by the grant Sc. Sc. 2628.2008.2, and by the program of the Presidium RAS ‘Quantum Physics of Condensed Matter’. VAT greatly thanks A Levanyuk for valuable discussions.

#### References

- [1] Müller K A and Burkard H 1979 *Phys. Rev. B* **19** 3593
- [2] Stokowski S E and Schawlow A L 1969 *Phys. Rev.* **178** 464
- [3] Vikhnin V, Trepakov V, Smutný F and Jastrabík L 1996 *Ferroelectrics* **176** 7
- [4] Trepakov V A, Kapphan S E, Bednorz J G, Gregora I and Jastrabík L 2004 *Ferroelectrics* **304** 83
- [5] Feofilov S P, Kaplyanskii A A, Kulinkin A B, Mikhailov P A and Zakharchenya R I 2007 *J. Lumin.* **122/123** 740
- [6] Petrykin V and Kakihana M 2005 *Sol–Gel Processing (Handbook of Sol–Gel Science and Technology: Processing, Characterization and Applications vol 1, ed H Kozuka) ed S Sakka* (New York: Kluwer Academic) pp 77–104
- [7] Wendlandt W W and Hecht H G 1966 *Reflectance Spectroscopy* (New York: Wiley)
- [8] Howard S A, Yau J K and Anderson H U 1989 *J. Appl. Phys.* **65** 1492
- [9] Wu X W and Liu X J 2007 *J. Lumin.* **122/123** 869
- [10] Makarova M V, Kazin P E, Zaitsev D D, Eremina N S, Tret'yakov Yu D and Jansen M 2003 *Inorg. Mater.* **39** 614
- [11] Cardona M 1965 *Phys. Rev.* **140** A651
- [12] van Benthem K, Elsässer C and French R H 2001 *J. Appl. Phys.* **90** 6156
- [13] Kahn A H and Leyendecker A J 1964 *Phys. Rev.* **135** A1321
- [14] Basun S A, Bianchi U, Bursian V E, Kaplyanskii A A, Kleemann W, Sochava L S and Vikhnin V S 1996 *J. Lumin.* **66/67** 526
- [15] Bickel N, Schmidt G, Heinz K and Müller A K 1989 *Phys. Rev. Lett.* **62** 2009
- [16] Chang W, Kirchoefer S W, Pond J M, Bellotti J A, Qadri S B, Haeni J H and Schlom D G 2004 *J. Appl. Phys.* **96** 6629
- [17] Pertsev N A, Tagantsev A K and Setter N 2000 *Phys. Rev. B* **61** R825
- [18] Kittel C 1946 *Phys. Rev.* **70** 965
- [19] Naumov I and Bratkovsky A M 2008 *Phys. Rev. Lett.* **101** 107601